J Low Temp Phys (2015) 179:126–137
DOI 10.1007/s10909-014-1228-z

Entropy Bottlenecks at T → 0 in Ce-Lattice and Related Compounds

Julian G. Sereni

Received: 21 July 2014 / Accepted: 6 September 2014 / Published online: 20 September 2014

Abstract A number of specific heat C_m anomalies are reported in Ce- and Yb-lattice compounds around 1 K which cannot be associated to usual phase transitions despite of their robust magnetic moments. Instead of a $C_m(T)$ jump, these anomalies show coincident morphology: (i) a significant tail in C_m/T, with similar power law decay above their maxima ($T > T_m$), (ii) whereas a $C_m(T^2)$ dependence is observed below T_m. (iii) The comparison of their respective entropy gain $S_m(T)$ indicates that $\approx 0.7R\ln 2$ is condensed within the $T > T_m$ tail, in coincidence with an exemplary spin-ice compound. Such amount of entropy arises from a significant increase of the density of low energy excitations, reflected in a divergent $C_m(T > T_m)/T$ dependence. (iv) Many of their lattice structures present conditions for magnetic frustration. The origin of these anomalies can be attributed to an interplay between the divergent density of magnetic excitations at $T \to 0$ and the limited amount of degrees of freedom: $S_m = R\ln 2$ for a doublet-ground state. Due to this "entropy bottleneck," the paramagnetic minimum of energy blurs out and the system slides into an alternative minimum through a continuous transition. A relevant observation in these very heavy fermion systems is the possible existence of an upper limit for $C_m/T_{\mathrm{Lim}T\to 0} \approx 7$ J/mol K^2 observed in four Yb- and Pr-based compounds.

Keywords Heavy fermions · Specific heat anomalies · Entropy

1 Introduction

Within the study of quantum critical phenomena, the search of magnetic systems tunable to low temperature transitions has provided valuable information about the

J. G. Sereni (✉)
Lab. Bajas Temperaturas, Centro Atómico Bariloche (CNEA), CONICET, I.B. (U.N.Cuyo),
8400 San Carlos de Bariloche, Argentina
e-mail: jsereni@cab.cnea.gov.ar

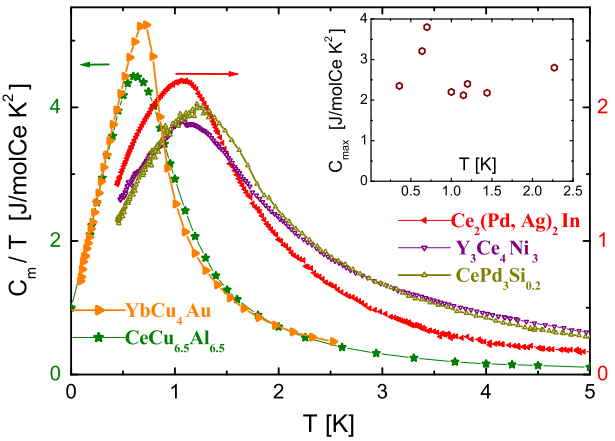

Fig. 1 Five examples of C_m/T anomalies around 1 K. *Left axis* $YbCu_4Au$ [9] and $CeCu_{6.5}Al_{6.5}$ [10]. *Right axis* $Ce_2(Pd_{0.5}Ag_{0.5})_2In$ [11], $Y_3Ce_4Ni_3$ [12], and $CePd_3Si_{0.2}$ [13]. *Inset* C_{max} values of samples included in this figure and in Fig. 2 (Color figure online)

physical properties of Ce and Yb compounds [1,2]. Those investigations have revealed the variety of alternative ground states that become accessible because of the subtle competition between comparable minima of energy. They may involve exotic or hidden phases arising from e.g., geometrical frustration [3,4], Griffith phases [5], dimers formation [6], or spin liquids [7]. Coincidentally, the knowledge of thermal properties in that region of temperature have shown the effects of thermodynamic constraints approaching quantum criticality at $T \to 0$ [8]. In this context, some similarities have been observed in Ce- and Yb-based systems around 1 K associated to specific heat (C_m) anomalies.

Five examples of those anomalies are collected in Fig. 1: $YbCu_4Au$ [9] and $CeCu_{6.5}Al_{6.5}$ [10] on the left axis, $Ce_2(Pd_{0.5}Ag_{0.5})_2In$ [11], $Y_3Ce_4Ni_3$ [12], and $CePd_3Si_{0.2}$ [13] on the right axis. These Ce- and Yb-lattice systems include different crystalline structures, stoichiometric compositions, Ce-ligand alloys, and interstitial atoms. The common features among them are the comparable values of their $C_m(T_m)$ maxima (see the inset in Fig. 1), followed by a monotonous decrease at $T > T_m$ without showing any discontinuity nor changes in their $\partial(C_m/T)/\partial T$ slopes.

The double logarithmic representation of C_m/T versus T presented in Fig. 2 shows their thermal dependencies above T_m following a power law with very similar exponents. In this figure other examples are included like the pseudo binary alloys $CeCu_{0.45}Si_{1.55}$, $CeCu_{0.75}Si_{1.25}$ [14], and the stoichiometric compound CeIrSi [15]. The $C_m/T|_{T>T_m}$ tail of all these systems are properly described by a modified power law: $C_m/T = g/(T^q + a)$ [17], with an exponent $q = 2 \pm 0.2$, whereas the parameter a ranges between zero and a few degrees. Another common feature among these systems is the $C_m \propto T^2$ dependence at $T < T_m$. The alloy $YbCu_{4.3}Au_{0.7}$ [16] is included in Fig. 2 as an illustrative comparison for the next section. This and its related $YbCu_{5-x}Au_x$ alloys (with $0.7 \geq x \leq 0.5$) also show power law $C_m/T|_{T>T_m}$ dependencies but with a concentration-dependent exponent $q(x)$ ($1.3 \geq q \geq 0.95$ [16]), whereas $a = 0$ in all of them. Nevertheless, the respective $C_m/T|_{T>T_m}$ tails

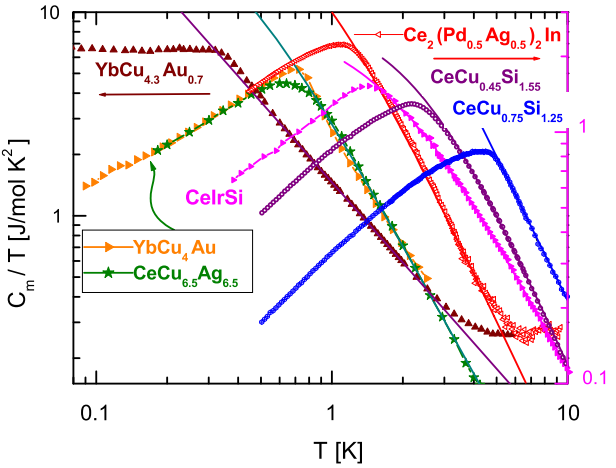

Fig. 2 Double logarithmic representation showing the power law dependencies of $C_m/T|_{T>T_m}$ versus T and $C_m|_{T<T_m} \propto T^2$ of $CeCu_xSi_{2-x}$ [14], CeIrSi [15] and $YbCu_{4.3}Au_{0.7}$ [16]. Continuous curves are fits with the $C_m/T = g/(T^q + a)$ function [17] (Color figure online)

scale each other as a function of T^q because they exhibit an isosbestic point [18] at $T \approx 1.8$ K. The relevant characteristic of this system is the constant, and very high value of $C_m/T|_{\mathrm{Lim}T\to 0} \approx 6.7$ J/mol K^2 which reveals an extremely high density of low energy excitations. Notice that, despite of the plateau observed in $C_m/T|_{\mathrm{Lim}T\to 0}$, a T_m maximum always occurs in $C_m(T)$.

The aim of this work is to determine whether the coincident features observed in these anomalies have a common origin and explore the nature of the underlying phenomena. For such a purpose, we first analyze the thermodynamic constraints imposed by the available degrees of freedom for a doublet-ground state (GS) system. The consequences of the paramagnetic phase instability are discussed in terms of the free energy competition with alternative minima.

2 Discussion

2.1 Analysis of the Entropy Gain

Valuable information for the study of this type of anomalies is provided by the thermal dependence of the magnetic entropy: $S_m = \int C_m/T \times dT$, presented in Fig. 3 after being normalized to the value of a doublet GS, $R\ln 2$. The respective extrapolations of $C_m/T\ |_{T\to 0}$ from the lowest measured temperatures to $T = 0$ were performed according to the $C_m(T^2)$ dependencies extracted from e.g., Fig. 2 for $T < T_m$. A relevant feature of the systems included in Fig. 3 is that the maximum slope of $\partial S_m/\partial T$ (i.e., the maximum of C_m/T) is reached at a nearly common value of $S_m \approx 0.3R\ln 2$. This means that all systems collect a similar amount of entropy at the respective T_m temperatures regardless their structure, Ce- or Yb-based composition, stoichiometric, or alloyed but always with a doublet GS. Searching for a possible meaning of such a coincidence, one finds that this value corresponds to the remanent entropy (S_0) of

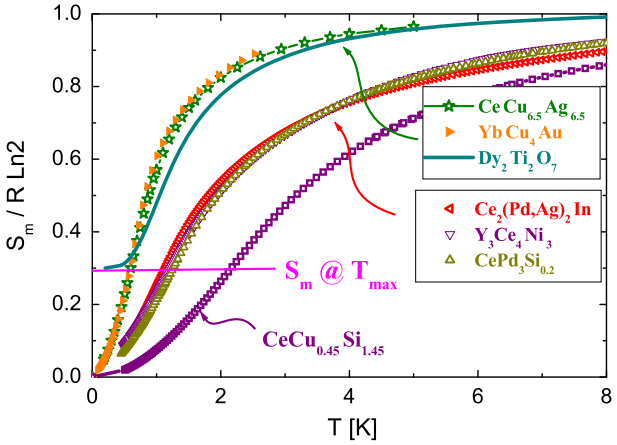

Fig. 3 Comparative evolution of the thermal dependence of the magnetic entropy (S_m) normalized to Rln2. The line at $S_m \approx 0.3R\ln 2$ indicates the entropy accumulated up to $T = T_m$. Continuous curve: $S_m(T)$ of the Spin Ice $Dy_2Ti_2O_7$ [19] included for comparison (Color figure online)

the well known spin-ice compound $Dy_2Ti_2O_7$ [19]. In order to compare this behavior with that of the systems under study, we have included its $S_m(T)$ dependence in Fig. 3 (continuous curve) taking into account that all systems coincide in entropy (Rln2) once both levels are equally occupied at high temperature, provided other crystal field levels are at much higher energy. Notice that the remanent entropy (S_0 at $T = 0$) of the spin-ice is related to an intrinsic geometrical frustration, which in other systems can be eventually dodge through different type of phase transitions like e.g., in Shastry-Sutherland lattices [20]. This coincidence in the entropy gain within the paramagnetic phase suggests that the large $C_m/T\ |_{T>T_m}$ tails in these systems may arise from frustration effects that inhibit the magnetic system to develop long-range order.

An illustrative analysis of the role of the entropy in the GS formation of these systems can be done comparing the $S_m(T)$ variation of stoichiometric $YbCu_4Au$ with the $YbCu_{4.3}Au_{0.7}$ alloy performed in Fig. 4. These related systems follow two different ways for $S_m(T) \to 0$ at $T = 0$. While stoichiometric $YbCu_4Au$ (with a cusp at C_m/T_m) shows a positive curvature $\partial^2 S_m/\partial T^2|_{\mathrm{Lim}T\to 0} > 0$, $YbCu_{4.3}Au_{0.7}$ ends with $\partial^2 S_m/\partial T^2 = 0$ as a consequence of the plateau observed at $C_m/T|_{\mathrm{Lim}T\to 0}$. In the figure, the dashed (cyan) curve represents the $S_{PL} = \int 3.1/(T^{2.1}+0.1)\times dT$ function, computed using the power law fit to $C_m/T\ |_{T>T_m}$ of $YbCu_4Au$. As expected, the S_{PL} curve deviates from the measured $S_m(T)$ at T_m and crosses the $S_m = 0$ axis at finite temperature, because it exceeds the $S_m = R\ln 2$ physical limit due to its divergent character at $T \to 0$. Although less pronounced, a similar feature is observed for $YbCu_{4.3}Au_{0.7}$, where the continuous (red) curve represents the $S_{PL} = \int 1.46/T^{1.3}\times dT$ dependence extracted for this alloy. In this case, the deviation of computed entropy from the measured $S_m(T)$ occurs at lower temperature because of the slower increase of the excitations density at low energy.

Notice the subtle crossing between $S_{PL}(T)$ and $S_m(T)$ in $YbCu_{4.3}Au_{0.7}$ that produces a slight discontinuity in the $\partial S_m/\partial T$ slope according to the fact that the $S_m(T)$

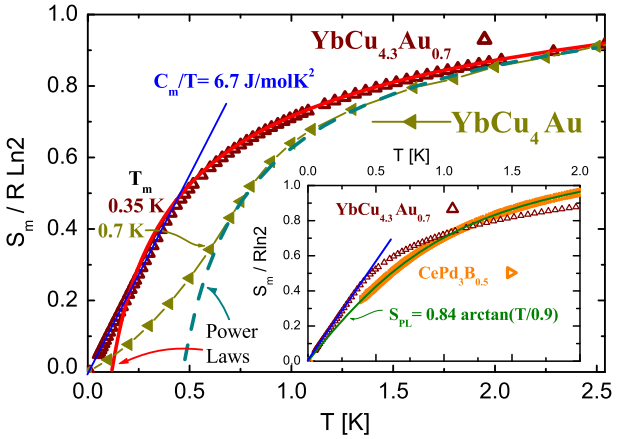

Fig. 4 Comparison between two isotypic Yb compounds. *Dashed* (*cyan*) and *continuous* (*red*) *curves* computed from respective $C_m/T\ |_{T>T_m}$ power laws. *Straight (blue) line* represents the $S_m(T < T_m)$ region. *Inset* Comparison between $YbCu_{4.3}Au_{0.7}$ and $CePd_3B_{0.5}$, *continuous (green) curve* represents the analytical fit (Color figure online)

gain up to $T_m \approx 0.4$ K is not tangent to S_{PL}. Although from thermodynamics a change of slope in the $\partial S_m/\partial T$ derivative corresponds to a second-order transition, the magnitude of the observed discontinuity is practically irrelevant, i.e., less that 10 % of the value predicted for a second-order transition in the mean field for a spin $s = 1/2$ [21]. This discontinuity even disappears for $YbCu_{4.6}Au_{0.4}$ [16].

Concerning the $YbCu_4Au$ compound, it is evident that the measured $S_m(T)$ deviates from the negative $\partial^2 S_{PL}/\partial T^2|_{T>T_m} < 0$ curvature, because the divergent character of C_m/T would end into a non physical singularity at $T = 0$. Consequently, the negative curvature of $S_m(T)$ itself becomes non physical and contrary to the third law of thermodynamics for $T \to 0$ [22]. One should remark that, in a classical second-order transition, the $S_m(T \to 0)$ extrapolation from the paramagnetic phase joins the one performed from the ordered phase at $T = 0$, with the consequent compensation expected for the entropy as a *state quantity*. This is not the case for the studied compounds, because no entropy compensation is possible since the magnetic *entropy bottleneck* produced by the $S_m = R\ln 2$ limit impedes such a compensation.

2.2 Maximum Value of $\gamma|_{T\to 0}$

Coming back to the $\partial^2 S_{PL}/\partial T^2|_{T>T_m} = 0$ case, the divergent $C_m/T\ |_{T\to 0} = \gamma_{T\to 0}$ behavior results in an exceptionally high value of ≈6.7 J/mol K^2 as observed in $YbCu_{5-x}Au_x$ within the $0.7 \geq x \geq 0.5$ range [16]. The fact that this value is independent of concentration below T_m and nearly coincides with other very heavy Fermions, arises the question whether it represents an upper limit for the density of excitations approaching $T = 0$. Those compounds are YbBiPt [23], $YbCo_2Zn_{20}$ [24] and $PrInAg_2$ [25], whose $\gamma_{T\to 0}$ values are ≈ 7.3 J/mol K^2 for Yb-based compounds and $\gamma_{T\to 0} \approx 6.5$ J/mol K^2 for $PrInAg_2$. Notably, the latter compound has a non-Kramer

doublet GS [25] because of its integer $J = 4$ total angular momentum. Concerning Ce-based compounds, to our knowledge the highest value is reported for $CeNi_9Ge_4$ with $\gamma_{T\to 0} \approx 5.6$ J/mol K^2 [26], followed by $CePd_3B_{0.5}$ [27] with a slightly lower value of $\gamma_{T\to 0} \approx 5.3$ J/mol K^2 extrapolated from $T > 0.45$ K, see below.

Another interesting question arises concerning the nature of the $\gamma_{T\to 0}$ plateau, because it could be associated to the formation of an extremely narrow band or it simply reflects a discrete spectrum of constant density of low energy excitations. The $C_m/T\ |_{T\to 0}$ evolution in $CePd_3B_{0.5}$ provides significant information, because it is a unique case showing a monotonous temperature dependence, described by $C_m/T = 4.3/(T^2+0.8)$ over a decade of temperature [27]. This function extrapolates to $T = 0$ with signatures of Fermi liquid (FL) behavior because for $T << 0.8$ K it can be written as $5.4(1 - T^2/0.8)$, that is the specific heat expansion for a Fermi gas [28].

In the inset of Fig. 4 the low temperature $S_m(T)$ of $YbCu_{4.3}Au_{0.7}$ and $CePd_3B_{0.5}$ are compared, showing that the latter is the only case where $S_m(T)$ and its second derivative tend to zero monotonously. Since for this case the lower limit of the experimental results is $T \approx 0.45$ K, the continuous curve extrapolated to $T = 0$ is computed from $S_{PL} = \int 4.3/(T^2 + 0.8) \times dT$ (dark green in the inset of Fig. 4). Interestingly, in the case of $CePd_3B_{0.5}$ that follows a $C_m/T \propto 1/T^2$ dependence, S_{PL} can be evaluated analytically by the formula $\int dx/(x^2 + c) = (1/c) \times \arctan(2x/c)$ [29]. The $S_{PL} = 0.83 \times \arctan(x/0.9)$ curve is the one depicted in the inset of Fig. 4 for $CePd_3B_{0.5}$ after normalized by $R\ln 2$. As expected, $\arctan x \to x$ as $x \to 0$, fulfilling the condition for a FL system. Very low temperature electrical resistivity measurements are certainly required to confirm the FL nature of this GS.

2.3 Analysis of the Free Energy Minima

The search of the origin of these anomalies requires a detailed analysis of the evolution of free energy minimum. The lack of a jump associated to the $C_m/T(T)$ anomalies included in Figs. 1 and 2 indicates that no second-order transition occurs rather a continuous modification in the landscape of the free energy surface. A possible description for this situation is sketched in Fig. 5 where competing minima in the Gibbs energy (G) is illustrated. On the left panel, Fig. 5a represents the Gibbs surface for the paramagnetic ($T > T_m$) phase, with the (yellow) disk indicating the G minimum and the arrows two alternative paths to energetically neighbors minima, and Fig. 5b the situation for $T < T_m$, where the system (yellow disk) has moved into another minimum of G because the former has vanished. On the right panel, Fig. 5c presents a schematic comparison of the $G(\Psi)$ dependencies at $T > T_m$, $T = T_m$ and $T < T_m$ being Ψ a generic order parameter.

Differently than in a second-order transition, where the paramagnetic $G(\Psi = 0)$-minimum continuously transforms into a $G(\Psi \neq 0)$ one as Ψ starts to grow from zero, in this case the G-minimum of the paramagnetic phase is blurred out by the *entropy bottleneck* originated in the divergent growth of the density of excitations. Since that minimum is no workable anymore for $T \leq T_m$, the system slides along the free energy surface into any other accessible minimum as represented in Fig. 5c for $T = T_m$.

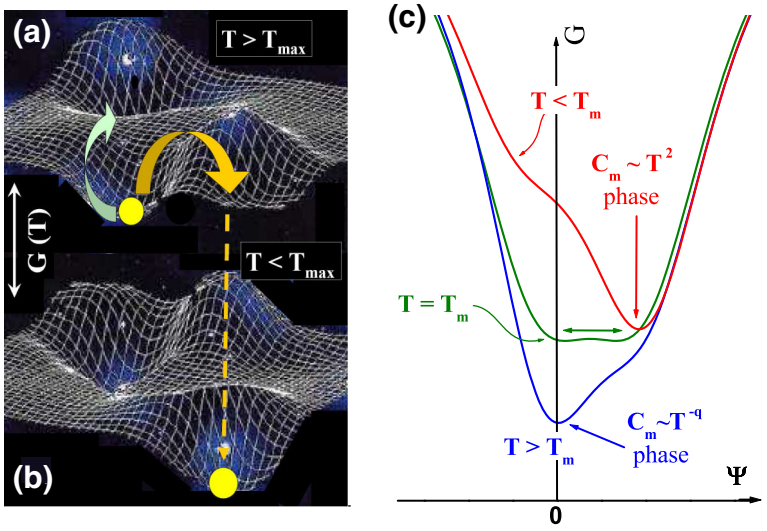

Fig. 5 Schematic representation of competing alternative minima of Gibbs free energy (G). **a** At $T > T_m$ the *yellow disk* indicates the paramagnetic minimum of G and the *arrows* the way to two alternative minima. **b** At $T < T_m$ the *yellow disk* indicates the chosen minimum of G once the paramagnetic one was blurred out. **c** Description of $G(\Psi, T)$ variation (where Ψ is a generic order parameter) for three representative temperatures to show how the $G(T > T_m)$ minimum of the paramagnetic phase (at $\Psi = 0$, *blue curve*) blurs out and the system slides at $T = T_m$ (*green curve*) into an alternative minimum at $\Psi \neq 0$ for $T < T_m$ (*red curve*) (Color figure online)

As mentioned in the description of Fig. 3, one of the common features among these compounds is the coincident amount of the entropy collected up to T_m: $S_m \approx 0.3R\ln 2$, that also coincides with the remanent entropy of the spin-ice compound $Dy_2Ti_2O_7$. Therefore, frustration effects which inhibit any order parameter development have to be taken into account as the origin of the entropy accumulated at $T > T_m$. In fact, many of the analyzed systems crystallize in structures favoring geometrical frustration, like tetrahedral nearest neighbors coordination in $YbCu_4Au$ and CeIrSi, or triangular one in $Ce_2(Pd_{0.5}Ag_{0.5})_2In$, $Y_3Ce_4Ni_3$, and $CeCu_{0.45}Si_{1.55}$. The fact that the entropy condensed above T_m compares with that of $Dy_2Ti_2O_7$ indicates that these systems can dodge an intrinsically degenerated GS sliding into an alternative minimum of energy once they have condensed such amount of entropy. This *entropy bottleneck* seems to properly represent a thermodynamical constraint which leads the systems to resolve their magnetic frustration accessing to alternative (previously hidden) phases.

2.4 About the Nature of the Anomaly

Before discussing these anomalies as originated in a peculiar phase transition, it is illustrative to compare their morphology with those of other well-known anomalies. One of the systems included in Fig. 6 is $CeCu_{6.5}Al_{6.5}$ whose anomaly was compared in the literature with a Schottky type anomaly [10]. Although its $C_m(T_m) \approx 3.3$ J/mol K value is close to the value for two equally degenerated levels (i.e., 3.64 J/mol K),

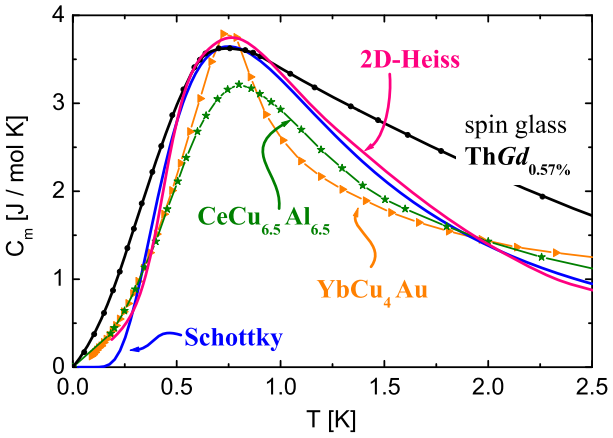

Fig. 6 Comparison of $YbCu_4Au$ and $CeCu_{6.5}Al_{6.5}$ anomalies with Schottky, spin glass, and 2D-simple quadratic Heisenberg lattice anomalies (Color figure online)

the observed thermal dependencies above and below T_m do not fit into such a class of anomalies. The same analysis applies to $YbCu_4Au$ also included in Fig. 6. Additionally to the $C_m(T)$ dependence, the other systems studied in this work show much lower $C_m(T_m)$ maximum as it can be seen in the inset of Fig. 1.

A similar comparison can be done with the specific heat anomaly of spin glasses. Also in this case the $C_m \propto T^2$ temperature dependence displayed by the compounds included in Fig. 2 below T_m suggests a quasi-two-dimensional (2D) magnetism [30] rather than a spin glass-like behavior (c.f. $C_m \propto T$ [31]). Additionally, the observed power law $C_m(T)/T$ dependence for $T > T_m$ also differs form that of a spin glass, see in Fig. 6 the comparison with ThGd spin glass [32]. Furthermore, the lattice distribution of magnetic Ce and Yb atoms, including stoichiometric compounds, practically excludes any role of random interactions due to atomic disorder in this peculiar behavior.

Exploring a possible quasi-two-dimensional (2D) magnetic character for these systems, one finds that a simple quadratic lattice of Heisenberg spins 1/2 does not order magnetically, but at low temperature it tends to a $C_m \propto T^2$ dependence [33]. However, the $C_m/T\ |_{T>T_m}$ tail does not follow a power law like the one observed in the analyzed systems, also included in Fig. 6. Nevertheless, the entropy condensed at T_m coincides with the value observed in the systems under study, i.e., $S_m(T_m) \approx 0.3R\ln 2$ [34]. A spin liquid character for the GS for these systems has to be taken into account because that type of behavior was claimed for the triangular lattice organic materials ET and Pd(dmit)2 compounds showing a $C_m \propto T^2$ dependence [35] and the isotypic compound Yb_2Pt_2Pb [36].

A clear distinction between usual magnetic disorder effects in a magnetic lattice and the anomalies under study is provided by the family of $Ce_2(Pd_{1-x}Ag_x)_2In$ alloys. This system shows a ferromagnetic transition T_C decreasing in temperature and intensity from $T_C = 4.1$ K at $x = 0$ [37] down to ≈ 2 K at $x = 0.4$, where the ferromagnetic transition vanishes. In coincidence with the progressive reduction of the $C_m(T_C)$ jump, another anomaly arises at $T_m \approx 1.1$ K, becoming fully developed at $x = 0.5$ as

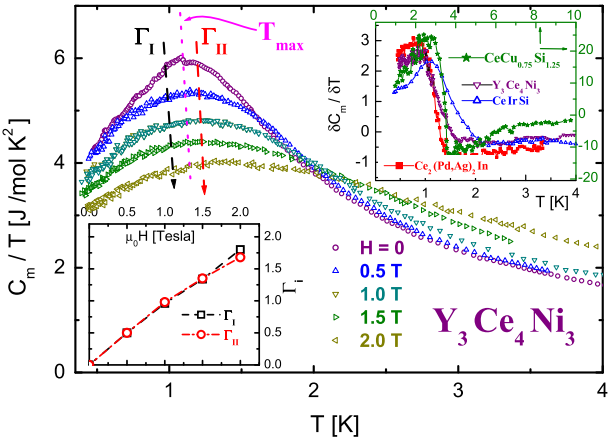

Fig. 7 Magnetic field effect on the $C_{\mathrm{m}}/T(T)$ dependence of $Y_3Ce_34Ni_3$. Γ_I and Γ_{II} indicate the C_m/T values on respective sides of the transition. *Lower inset* Field dependence of Γ_I and Γ_{II} evaluated at $\pm 10\%$ of T_{m}. *Upper inset* Discontinuity of the specific heat derivative in four of the systems under analysis (Color figure online)

depicted in Figs. 1 and 2 . Disorder effects produced by Ag doping the Pd lattice may explain the broadening and weakening of the ferromagnetic transition, but not the emerging anomaly at T_{m} as an independent entity.

Due to the low temperature range at which these anomalies occur, quantum fluctuation effects should not be excluded. This fact is supported by the analysis of magnetic phase diagrams performed on Ce systems, whose order transitions are driven to $T < 1$K by alloying Ce-ligand atoms [8,17]. In those cases, a systematic change of the phase boundary slope between 2 and 3 K is observed and attributed to quantum fluctuations overcoming the decreasing thermal fluctuations. Additionally, the possible 2D character of those fluctuations was determined by neutron scattering studies performed on the archetype of non-Fermi-liquid systems, $CeCu_{6-x}Au_x$ [38]. Nevertheless, one has to remak that microscopic quantum critical mechanisms and thermodynamic constraints do not exclude each other because they produce intertwined effects.

Focusing on the thermodynamic conditions derived from an *entropy bottleneck*, one has to analyze how the access to an alternative minima of energy occurs. From the discussion held in §2.3, the slide of the system into another minimum is expected to be continuous according to the lack of an energy threshold once the paramagnetic minimum was blurred. In terms of free energy, such type of crossover into another minimum is associated to a discontinuity in its third derivative, i.e., $\partial^3 G/\partial T^3$, which corresponds to a third-order transition according to the Ehrenfest definition. Taking profit from Pippard's description [39] of third order transitions, the occurrence of that class of transition can be tested applying that criterion of the $\partial C_{\mathrm{m}}/\partial T$ derivative discontinuity. Such a discontinuity is clearly observed in the four systems included in the upper inset of Fig. 7. The broadness of the transitions can be attributed to the polycrystalline body of the samples.

A complementary analysis concerning the nature of this anomaly can be performed exploring the G-derivatives involving other intensive parameters, e.g., pressure (P) or magnetic field (H). In a third-order transition, the equality between phases I and II

corresponds to the respective entropy derivatives:

$$\partial S_I(T, H)/\partial T = \partial S_{II}(T, H)/\partial T$$

For simplicity, we define $\partial S/\partial T(= C_{\rm m}/T)=\Gamma$, then the equality becomes $\Gamma_I=\Gamma_{II}$ with the discontinuity in its derivative. An equivalent formulation of Clapeyron's equation [39] for Ehrenfest third-order transition can be written as:

$$dT/dH = [(\partial\Gamma_{II}/\partial H)_T - (\partial\Gamma_I/\partial H)_T]/[(\partial\Gamma_I/\partial T)_H - (\partial\Gamma_{II}/\partial T)_H]$$

In the case of an equal variation of $\Gamma_i(H)$ on both sides of the transition, i.e., $(\partial\Gamma_{II}/dH) = (\partial\Gamma_I/dH)$ one extracts that $dT/dH = 0$. This implies no change of the transition temperature under field variation as it is observed in Fig. 7 for $Y_3Ce_4Ni_3$. The variation of $\Gamma_i(H)$ on respective sides of the transition are compared in the lower inset of that figure. Notice that the $\Gamma_I(H) = \Gamma_{II}(H)$ equality holds up to $H = 1.5$ Tesla because above that value the magnetic field induces an incipient ferromagnetic character. Notice that this compound also fulfills some conditions for magnetic frustration like a triangular arrangement of its magnetic atoms [40] and a large frustration factor [3] $f = -\theta/T_{\rm m}$ with $f > 30$, although crystal field effects may contribute significantly to this value. Despite of the scarce available examples of specific heat studies under pressure, the case of $CeAl_3$ [41] is a good candidate for this analysis because the anomaly at $T_{\rm m} = 0.35$ K is suppressed with 0.38 kbar.

3 Conclusions

The number of Ce- and Yb-lattice compounds showing specific heat anomalies around 1 K, with peculiar but similar temperature dependencies that cannot be associated to Schottky, spin-glass or 2D-systems anomalies, arises the question about which type of physics underlies that common behavior. The coincident entropy condensed into the $C_{\rm m}/T\ |_{T>T_{\rm m}}$, $S_m \approx 0.7R\ln 2$, resembles that of a geometrically frustrated spin-ice suggesting frustration as a factor to inhibit magnetic order development at $T > T_{\rm m}$. Crystal structures of many of those systems favor that possibility, particularly in stoichiometric compounds where disorder should play a minor role.

Such amount of entropy represents a sort of *entropy bottleneck* produced by a (power law) divergent growth of the density of magnetic excitations and the constraint imposed by the limited amount of available degrees of freedom: $R\ln 2$. Differently than in a Spin-Ice scenario, these systems are able to dodge that type of degenerated ground state by sliding into an alternative minimum of energy through a continuous transition with characteristics of third order.

The systematic $C_m \propto T^2$ dependence observed below T_m can be associated to a quasi-two-dimensional system. However, a direct determination of the magnetic structure and its dynamic nature requires of spectroscopic studies. A relevant feature extracted from this study concerns the possible existence of an upper limit of $C_{\rm m}/T_{{\rm Lim}T\to 0} \approx 7$ J/mol K^2. This value was systematically observed in at least four

Yb- and Pr-based compounds associated to a constant density of magnetic excitations at $T \to 0$. Nevertheless, constant $C_m/T_{\mathrm{Lim}T\to 0}$ does not necessarily imply the formation of an extremely narrow band like in the possible ground state of $CePd_3B_{0.5}$.

Acknowledgments The author is grateful to E. Bauer, I. Curlik, E.-W. Scheidt, and I. Zeiringer for allowing to access to original results, and M. Giovannini, M. Gómez Berisso, J.-P. Kappler, G. Nieva, P. Pedrazzini and G. Schmerber for experimental collaboration. This work was partially supported by project UNCuyo 06/C457.

References

1. G.R. Stewart, Rev. Mod. Phys. **73**, 797 (2001)
2. H.V. Löhneysen, A. Rosch, M. Vojta, P. Wölfle, Rev. Mod. Phys. **79**, 1015 (2007)
3. A.P. Ramirez, Annu. Rev. Mater. Sci. **24**, 453 (1994)
4. C. Lacroix, J. Phys. Soc. Jpn **79**, 011008 (2010)
5. T. Vojta, J. Schmalian, arXiv:cond-mat/0405609 (2004)
6. S. Miyahara, K. Ueda, Phys. Rev. Lett. **82**, 3710 (1999)
7. T. Radu, Y. Tokiwa, R. Coldea, P. Gegenwart, Z. Tylczynski, F. Steglich, Sci. Technol. Adv. Mater. **8**, 406 (2007)
8. J.G. Sereni, Phil. Mag. **93**, 409 (2013)
9. M. Galli, E. Bauer, St Berger, Ch. Dusek, M. Della Mea, H. Michor, D. Kaczorowski, E.W. Sheidt, F. Mirabelli, Physica B **312–313**, 489 (2002)
10. U. Rauchschwalbe, U. Gottwick, U. Ahlheim, H.M. Mayer, F. Steglich, J. Less-Common Metals **111**, 265 (1985)
11. M. Giovannini, private communication
12. O. Trovarelli, J.G. Sereni, G. Schmerber, J.P. Kappler, J. Magn. Magn. Mater. **140–145**, 1211 (1994)
13. G. Nieva; PhD Thesis, Univ. Nac. de Cuyo, 1988 (unpublished).
14. R. M-Reisener, Diplomarbeit, Tech. Hohschule Darmstdt, 1995 (unpublished).
15. F. Kneidingers, PhD Thesis, Technical University Vienna, 2014 (unpublished).
16. I. Curlik, M. Reiffers, J.G. Sereni, M. Giovannini, S. Gabani, arXiv:condmat.str/1403.6004v1 (2014)
17. J.G. Sereni, J. Low Temp. Phys. **147**, 179 (2007)
18. D. Vollhardt, Phys. Rev. Lett. **78**, 1307 (1997)
19. A.P. Ramirez, A. Hayashi, R.J. Cava, R.R. Siddharthan, B.S. Shastry, Nature **399**, 333 (1999)
20. S. Miyahara, K. Ueda, Phys. Rev. Lett. **82**, 3701 (1999)
21. P.H.E. Meijer, J.H. Colwell, B.P. Shah, Am. Jour. Phys. **41**, 332 (1973)
22. J.P. Abriata, D.E. Laughlin, Prog. Mater. Sci. **49**, 367 (2004)
23. Z. Fisk, P.C. Canfield, W.P. Beyermann, J.D. Thompson, M.F. Hundley, H.R. Ott, E. Felder, Phys. Rev. Lett. **67**, 3310 (1991)
24. M.S. Torikachvili, S. Jia, E.D. Mun, S.T. Hannahs, R.C. Black, W.K. Neils, D. Martien, S.L. Bud'ko, P.C. Canfield, PNAS **104**, 9960 (2007)
25. A. Yatskar, W.P. Beyermann, R. Movshovich, P.C. Canfield, Phys. Rev. Lett. **77**, 3637 (1996)
26. U. Killer, E.-W. Scheidt, W. Scherer, H. Michor, J. Sereni, Th Pruschke, Phys. Rev. Lett. **93**, 216404 (2004)
27. I. Zeiringer, J.G. Sereni, M. Gómez Berisso, K. Yubuta, P. Rogl, A. Grytsiv, E. Bauer, Mater. Res. Express **1**, 016101 (2014)
28. E.C. Stoner, Proc. Roy. Soc. (Lond) **A154**, 656 (1936)
29. see for example: M. Abramowitz, I.A. Stugun, *Handbook of Mathematical Functions* (Dover Publisher, New York, 1970)
30. see for example: A. Tari, *The Specific Heat of Mater at Low Temperatures* (Imperial College Press, London, 2003)
31. see for example: J.A. Mydosh, *Spin Glasses: An Experimental Introduction* (Taylor and Francis, London, 1993)
32. J.G. Sereni, T.E. Huber, C.A. Luengo, Sol. State Commun. **29**, 671 (1979)
33. J.L. De jongh, A.R. Miedema, Adv. Phys. **23**, 1 (1974)
34. D. Garcia, Using Monte Carlo Simulation, private communication

35. K. Kanoda, R. Kato, Annu. Rev. Condens. Matter Phys. **2**, 167 (2011)
36. M.S. Kim, M.C. Aronson, Phys. Rev. Lett. **110**, 017201 (2013)
37. M. Giovannini, H. Michor, E. Bauer, G. Hilscher, P. Rogl, T. Bonelli, F. Fauth, P. Fischer, T. Herrmannsdrfer, L. Keller, W. Sikora, A. Saccone, R. Ferro, Phys. Rev. B **61**, 4044 (2000)
38. H.V. Löhneysen, J. Magn. Magn. Mater. **200**, 532 (1999)
39. A.B. Pippard, *Elements of Classical Thermodynamics* (University Press, Cambridge, 1964)
40. R.B. Roof, A.C. Larson, D.T. Cromer, Acta Cryst. **14**, 1084 (1961)
41. G.E. Brodale, R.A. Fisher, N.E. Phillips, J. Flouquet, C. Marcenat, J. Magn. Magn. Mater. **54–57**, 419 (1986)